ТЕРМОДИНАМІЧНИЙ АНАЛІЗ ТА МОДЕЛЮВАННЯ

УДК 621.56/.59:[536.7:547.313.3]

Thermodynamic analysis of the ethylene reliquefaction system on LEG carriers when replacing throttle devices with ejectors

Larisa Morosuk[1], Victoriia Sokolovska-Yefymenko[2]✉, Volodymyr Ierin[3], Oleksandr Yefymenko[4], Andrii Moshkatiuk[5]

[1,2,4,5]Odesa National University of Technology, 112 Kanatnaya str., Odesa, 65039, Ukraine;

[3]NingboTech University, 1 Qianhu South Road, Ningbo, 315100, China

✉ e-mail: [2]kli24062006@gmail.com

ORCID: [1]http://orcid.org/0000-0003-4133-1984; [2]http://orcid.org/0000-0002-7275-5061; [3]http://orcid.org/0000-0001-7941-9725; [4]http://orcid.org/0000-0003-2571-9292; [5]http://orcid.org/0000-0003-3354-0321

LEG carriers' energy efficiency can be increased by improving the boil-off gas (BOG) reliquefaction installation processes in its components. In this study, it is proposed to replace the conventional reliquefaction process (CRP) of a LEG carrier "ANTIKITIRA" actual installation equipped throttle devices with an ejector reliquefaction process (ERP) having two-phase ejectors as expansion devices to increase the energy efficiency of the installation. Expansion devices $EV2^E$ and $EV2^R$ were replaced with two-phase ejectors in the proposed system. The ejector efficiencies are ensured by additional components (separators and the precooler in the bottoming stage of the cascade). Separators maintain a constant pressure at the compressor inlets, and the precooler reduces the load on the condenser-evaporator. An ejector model has been developed to analyze the proposed system. The design pressure at the ejector nozzle outlet is determined based on multivariate calculations. Energy and exergy analyses of ERP and CRP systems were carried out. According to the exergy analysis results, each component's influence on the energy efficiency of the CRP and ERP systems is estimated. The exergy losses in each ERP component are lower than the corresponding values in the CRP components. The exergy losses in the condenser and precooler of the CRP system are lower than in the ERP system. The total power consumption is the same in both cycles, and the cooling capacity of the ERP cycle has increased by 29.1 kW. Replacement of throttle devices led to a decrease in absolute exergy loss from 9.75 to 4.95 kW. The energy efficiency of the ERP cycle increased by 24%, and the exergy efficiency increased by 16%. The most significant exergy losses in both cycles are observed during compression in a two-stage cargo compressor of the bottoming stage of the cascade (29.0-34.1%). It is concluded that the proposed ERP cycle meets IMO requirements for vessel energy efficiency but requires additional capital investments.

Keywords: *Ethylene; Ejector; Exergy analysis; Reliquefaction installation*

doi: https://doi.org/10.15673/ret.v59i1.2618

Nomenclature:

e – specific exergy, kJ kg^{-1};
$\dot{E}$ – exergy, kW;
h – specific enthalpy, kJ·kg^{-1};
$\dot{m}$ – mass flow rate, kJ·kg^{-1};
$\dot{Q}$ – heat load, kW;
p – pressure, bar or MPa;
s – specific entropy, kJ·kg^{-1}·°C^{-1};
T – temperature, °C or K;
υ – velocity, m·s^{-1};
$\dot{W}$ – power, kW;
COP – coefficient of performance;

Δ – difference;
ε – exergy efficiency;
η – efficiency;
ω – entrainment ratio

Subscripts:
ad – adiabatic;
amb – ambient;
car – cargo;
c – compressor;
c-e – condenser-evaporator;
cond – condenser;
diff – diffuser;
e – evaporator, bottoming stage;
ec – economizer;
ej – ejector;
i – index of the component;
int – intermediate;
LPG – LPG heat exchanger;
mix – mixing;
nozz – nozzle;
pc – precooler;
r – topping stage;
scr – screw;
sep – separator;
tank – tank;
tot – total;
1-10, A, B – state of cycle

Superscripts:
CRP – conventional reliquefaction process;
E – ethylene;
ERP – ejector reliquefaction process;
EV – expansion valve;
in – inlet;
HS – high stage;
LS – low stage;
out – outlet;
R – propylene;
tank – tank;
tot – total

1. Introduction

Climate change, geopolitics, COVID-19, and military conflicts have affected people's lives and led to a global energy crisis. Liquefied gases as an alternative fuel play a leading role in mitigating the impact on the energy industry. In the present time, the transporting of liquefied gases over long distances is carried out by gas carriers. The supply of gases in a liquefied state is more profitable since transporting the corresponding volumes of compressed gases requires huge material costs [1]. Depending on the type of transported gases, they are divided into several groups, among which an important place is occupied by liquefied ethylene, which has significant energy potential. In the transport classification, it represents the LEG (Liquefied Ethylene Gas) group. A significant increase in demand for ethylene in recent years has been observed in China and the Middle and Far East. About 85 million tons of ethylene are produced worldwide annually. However, since most of this production is disposed of close to its place, only 2.5 million tons can be transported by sea over long distances [2].

Ethylene has a normal boiling point of -104 °C. Its physical properties determine the cargo retention system on the vessel. During transportation, part of the cargo evaporates, which increases the pressure and temperature in cargo tanks. A gas liquefaction system is used on gas carriers to maintain the pressure and temperature within normal limits. The reliquefaction systems on vessels transporting ethylene use cascade refrigerating machines.

To comply with mandatory vessel energy efficiency standards, such as the Energy Efficiency Design Index (EEDI) and the Ship Energy Efficiency Management Plan (SEEMP), designers and shipbuilders face the problem of improving the energy efficiency of the reliquefaction system [3]. The problem's solution is achieved by improving the processes in its components and finding new design solutions for the installation components during the design and operation of the entire system. When analyzing the component LEG reliquefaction systems, many authors showed that significant irreversible losses are observed in throttle devices (expansion valves) [4-8]. Thus, one of the promising ways to increase the system's performance is to reduce these losses by using more efficient expansion processes.

Considering the above, this paper presents a study to improve the reliquefaction process's productivity using an ejector as an expansion device. The chosen topic of study is relevant from the point of view of the prospects for the development of maritime transport in compliance with IMO requirements regarding vessel energy efficiency.

2. Literature review and problem statement

The study of processes in LEG reliquefaction

systems has been published in the papers of scientific teams from different countries.

Li et al. considered the issues of increasing the energy efficiency of the ethylene reliquefaction installation [4]. Optimization of the existing cycle was carried out using thermodynamic analysis. The exergy losses of each component are considered, and the efficiency of using available energy is estimated. The optimization resulted in an increase in the exergy efficiency of the reliquefaction process by about 19.0%. The amount of circulating refrigerant in the system decreases by about 44.9% per hour. The boil-off gas (BOG) reliquefaction system on a LEG carrier was evaluated by Sokolovska-Yefymenko et al. [6]. The study uses the entropy-cycle method to determine irreversibilities in a cascade cycle. The study results showed that when designing cascade installations of liquefied ethylene, it is necessary to improve the design of expansion devices, particularly to replace the throttle valve with an ejector. Berlinck et al. analyzed the parameters of the reliquefaction installation of an LPG carrier with a capacity of 20 tons per day [9]. An experimental study of the installation and its thermodynamic analysis by the exergetic method were carried out. Chien and Shih performed a numerical simulation of the ethylene reliquefaction installation [10]. The simulation model was developed based on the law of energy and mass conservation, empirical ratios of heat transfer coefficients, the theory of heat exchangers and compressors, and thermophysical properties of working fluids. A parametric analysis of the entire reliquefaction installation was carried out. Nanowski proposed a project to optimize the reliquefaction processes for the ethylene reliquefaction system [11]. An exergy analysis of the system was carried out, and irreversible losses of each component were determined. The results showed that the exergy efficiency of the optimized reliquefaction process was 44.5%, while in the existing process, it was 37.4%. The consumption of refrigerant and seawater in the optimized process also decreased by about 44.8% and 27.1% per hour, respectively. It is proved that the energy consumption in the optimized process reduces by 16.2%. Tan et al. proposed to increase the energy efficiency of a cascade ethylene reliquefaction plant by using an ejector as an expansion device [7]. An ejector model is presented, and its optimal parameters are determined. The authors claim that the ejector application in a particular situation reduces energy consumption by 15.7-27.9 kW compared with traditional expansion devices. Three potential circuit solutions for the LEG liquefaction installation are considered by Tan et al. in [12]. The optimal design characteristics of the studied processes are determined. It is proposed to use the study results as reference information on the process selection in the reliquefaction plant for LEG vessels. The energy efficiency of the three modified cycles of the ethylene reliquefaction plant considered in [12] was evaluated by authors in [8]. The process parameters are optimized individually to minimize the system's energy consumption. The results showed that compressors and throttle devices observed the most significant exergy losses. Ouadha and Beladjine conducted a thermodynamic analysis of the ethylene reliquefaction plant with various hydrocarbon refrigerants in the upper cascade [5]. R600a is recognized as the best refrigerant in terms of energy efficiency, exergy efficiency, and energy consumption. The authors claim that using more efficient expansion devices can enhance the process of reliquefaction.

The ejector is defined as a promising replacement for throttle devices to improve cooling system characteristics [13-16]. Wongwises and Disawas investigated a refrigeration system using a two-phase ejector as an expansion device [17]. The ejector cycle showed a slight increase in COP compared to the conventional refrigeration cycle. The cascade cycles using an ejector have been investigated in some studies [18, 19]. Using an ejector in CO_2 cycles is also considered a promising way to increase the efficiency of the refrigeration cycle [21, 22].

A literature review has shown that the ejector application improves energy and exergy refrigeration system efficiency, and its use in the presented ethylene reliquefaction system is appropriate. To estimate the characteristics of such systems, the authors of this paper propose to use energy and exergy analyses. Such methods allow, along with energy efficiency assessment, to obtain the distribution of exergy losses over the refrigeration cycle components and evaluate the use of the ejector on the system parameters.

3. LEG reliquefaction system description

The schematic diagram of the proposed system is developed based on the conducted studies of the ethylene reliquefaction installation of the LEG carrier "ANTIKITHIRA" in actual operating conditions. The study results were presented by Sokolovska-Yefymenko et al. in [6]. The new research is supposed to

begin with considering the schematic diagram of the LEG carrier "ANTIKITHIRA" which is classified as a conventional reliquefaction process (CRP). The schematic diagram of the CRP system is shown in Fig. 1 [22]. Fig. 2 shows the thermodynamic cycle of the CRP system in the T-s diagram.

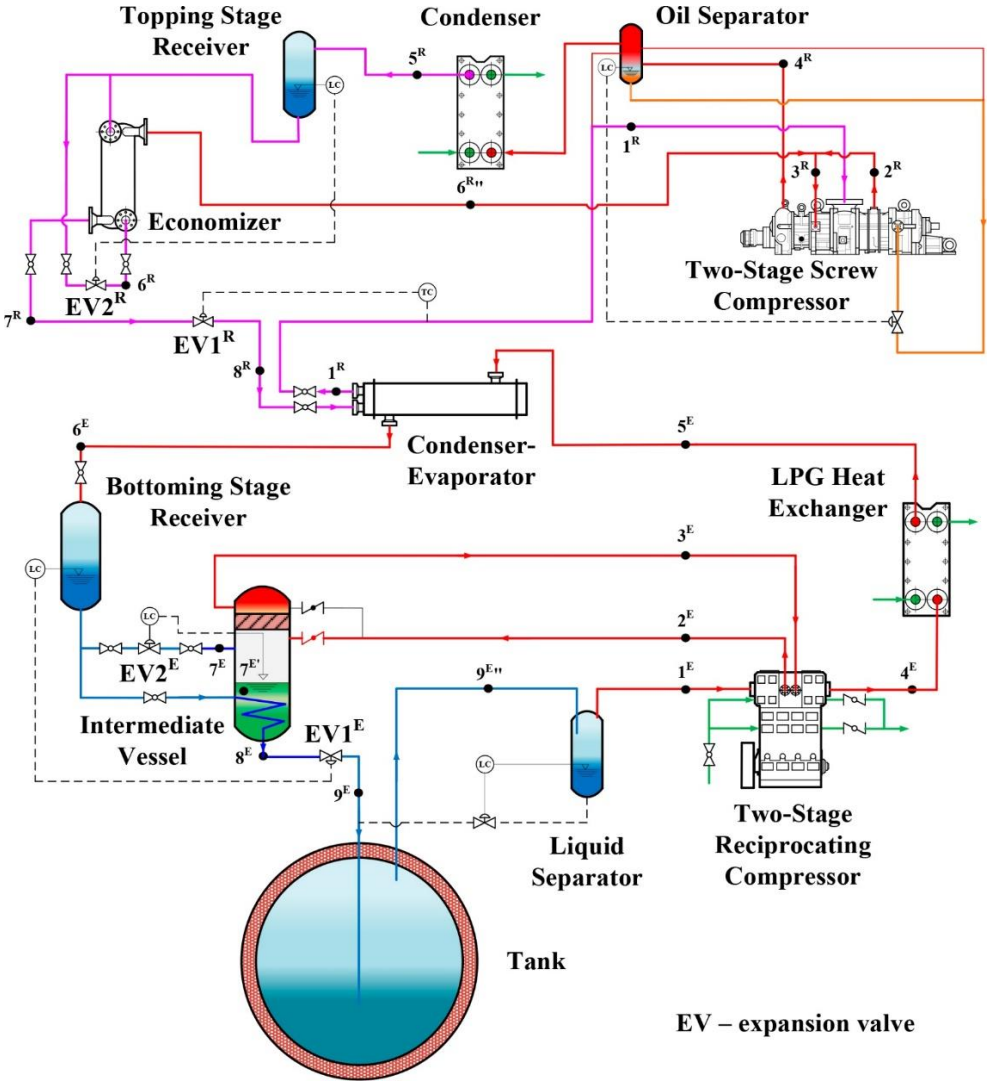

Figure 1 *– Schematic diagram of the CRP system [22]*

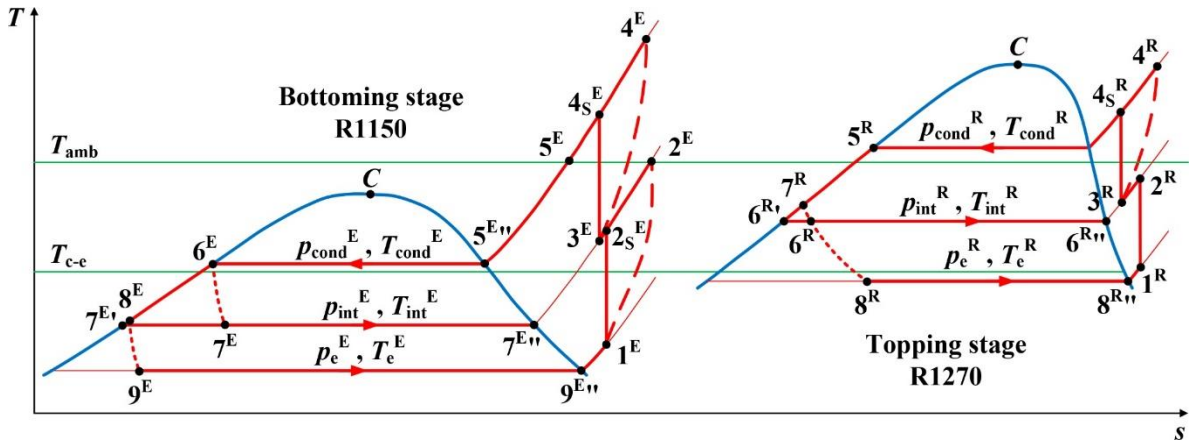

Figure 2 *– The thermodynamic cycle of the CRP system in the T-s diagram*

The novel schematic diagram provides for the throttle devices EV1R and EV2R replacement in the CRP system with two-phase ejectors classified as an ejector reliquefaction process (ERP). The replacement of throttle devices is accompanied by changes in the system schematic diagram (Fig. 3).

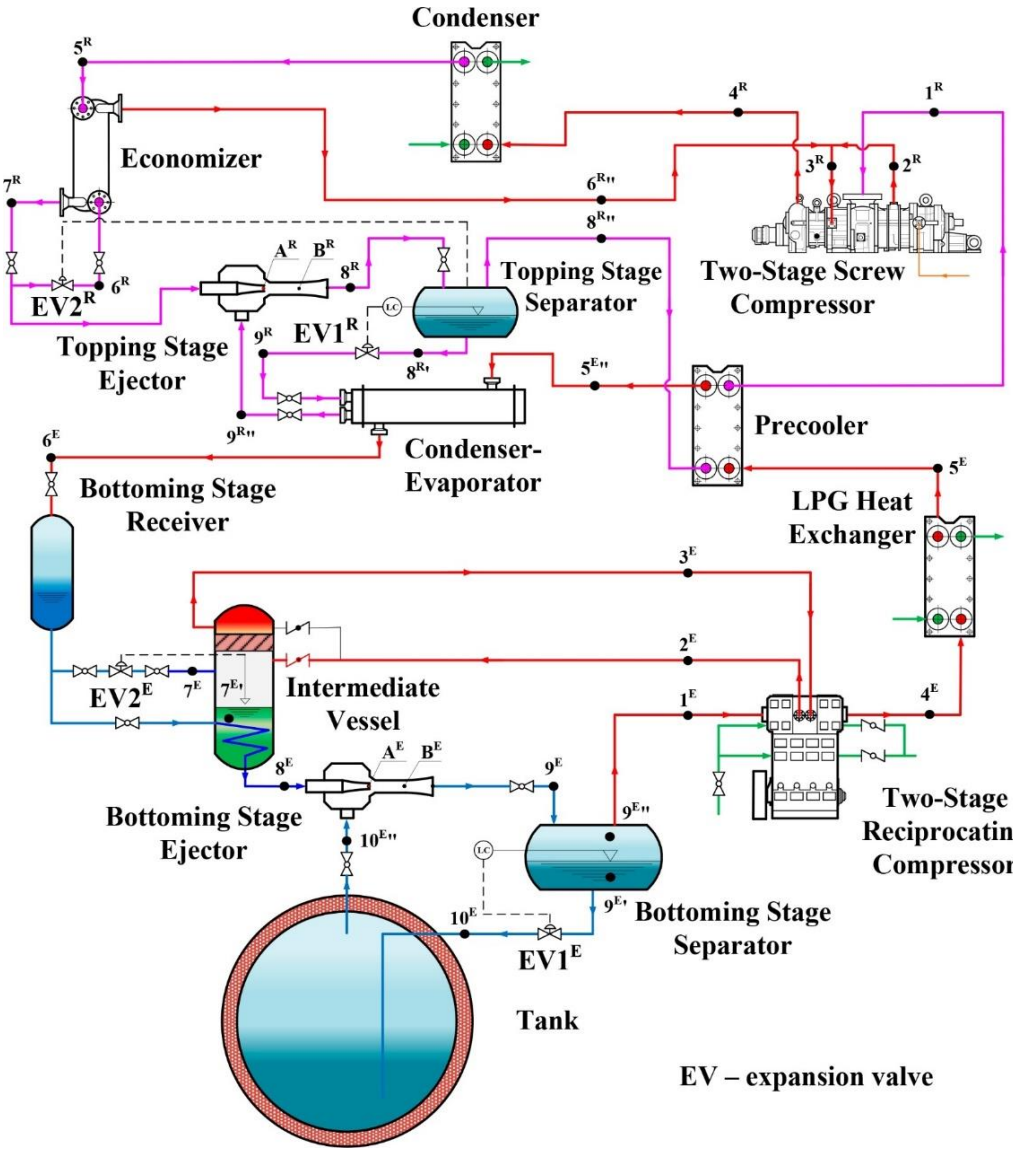

Figure 3 *– Schematic diagram of the ERP system*

The ERP system cycle includes the following processes.

The bottoming stage of the cascade operates at four pressure levels: the ethylene condensing pressure p_c^E, the intermediate pressure between the cargo reciprocating compressor stages p_{int}^E, the suction pressure in the low stage cylinder of the cargo reciprocating compressor p_e^{*E}, LEG storage pressure in tanks p_e^E.

Ethylene supercooled in the intermediate vessel coil (primary flow) with the mass flow rate $\dot{m}_e^{LS}$ (state 8^E) is sent to the bottoming stage ejector. In the ejector nozzle, the primary flow expands to the pressure p_e^E (state A^E). Due to the resulting discharge, the secondary flow of vapor ejected from the tank is sucked into the ejector suction chamber (state $10^{E"}$). In the ejector mixing chamber, both flows are mixed to the state of wet vapor (state B^E). Then the mixed flow is sent to the ejector diffuser, where the kinetic energy of velocity is converted into potential energy of pressure. At the ejector outlet, the pressure of the mixture (wet vapor) is p_e^{*E} (state 9^E). In the bottoming stage separator, the wet vapor is divided into saturated vapor (state $9^{E"}$) and saturated liquid (state $9^{E'}$). The saturated liquid expands in the expansion valve $EV1^E$ to the pressure of the p_e^E and is sent to the tank (state 10^E). Saturated vapor with the mass flow rate $\dot{m}_e^{LS}$ is directed to the suction line of the low stage of the cargo reciprocating compressor (state 1^E). After sequential compression in the cargo reciprocating compressor and cooling in the LPG heat exchanger (state 5^E), the superheated ethylene vapor is cooled to a saturated state in the precooler (state 5^{E*}). The resulting saturated ethylene vapor is completely condensed in the evaporator-condenser (state 6^E).

The topping stage of the cascade also operates at four pressure levels: the propylene condensing pressure p_c^R, the intermediate pressure between the screw

compressor stages p_{int}^{R}, the suction pressure in the low stage of the screw compressor $p_e{}^{*R}$, the evaporating pressure of propylene in the evaporator-condenser p_e^{R}.

The processes in the topping stage ejector are similar to those in the bottoming stage ejector. After the economizer, the primary flow of working fluid (state 7^{R}) enters the topping stage ejector, expands in the nozzle (state A^{R}), and takes the secondary flow of saturated vapor from the evaporator-condenser (state $9^{R''}$) into the suction chamber. The wet vapor with a pressure of p_e^{*R} is formed at the ejector outlet (state 9^{R}). The mixture flow is directed to the topping stage separator and is divided into saturated vapor (state $8^{R''}$) and saturated liquid (state $8^{R'}$). Saturated vapor superheats in the precooler (state 1^{R}) and enters the low stage of the screw compressor. After the topping stage separator, the saturated liquid expands in the expansion valve $EV1^{R}$ to the pressure p_e^{R} and evaporates in the evaporator-condenser.

4. Modeling of the ERP system

The processes of the proposed ERP system were modeled based on the mass and energy balance. The main operating pressures and temperatures were assumed to be the same as in the actual reliquefaction installation (in particular, tank pressure, condensing temperature, intermediate pressure, seawater temperature, etc.) [6].

The following assumptions to simplify the theoretical model of the proposed ERP system are used [6]:

– hydraulic losses in pipelines and heat losses in heat exchangers are not considered;

– the isentropic efficiency of the low stage of the cargo reciprocating compressor is 55%;

– the isentropic efficiency of the high stage of the cargo reciprocating compressor is 86%;

– the isentropic efficiency of the screw compressor is 86% (according to actual operating conditions).

4.1. Mathematical model of the ejector

The mathematical model of the ejector is developed based on the following assumptions:

– all types of heat losses are not considered;

– operating conditions are considered for a steady state;

– the effect of pressure drop on friction is neglected;

– a one-dimensional mixing model at constant pressure is used to evaluate the ejector performance;

– the efficiency of the nozzle (ηnozz) and diffuser (ηdiff) in the ejector is assumed to be 85%;

– it is assumed that the mixing efficiency ηmix is 95% [23];

– the secondary flow pressure drop and the velocity at the ejector inlet are neglected [24];

– the primary flow velocity at the ejector inlet is negligible;

– the secondary flow velocity is negligible compared to the primary flow velocity [24].

The method of computing the flow parameters in the ejectors of the bottoming and topping stages of the cascade consists in estimating the pressure at the diffuser outlet and the corresponding vapor quality and determining all other parameters based on these data. As an example, the bottoming stage ejector is considered. The schematic and structural diagram of the ejector and the working processes in the ejector are shown in Fig. 4.

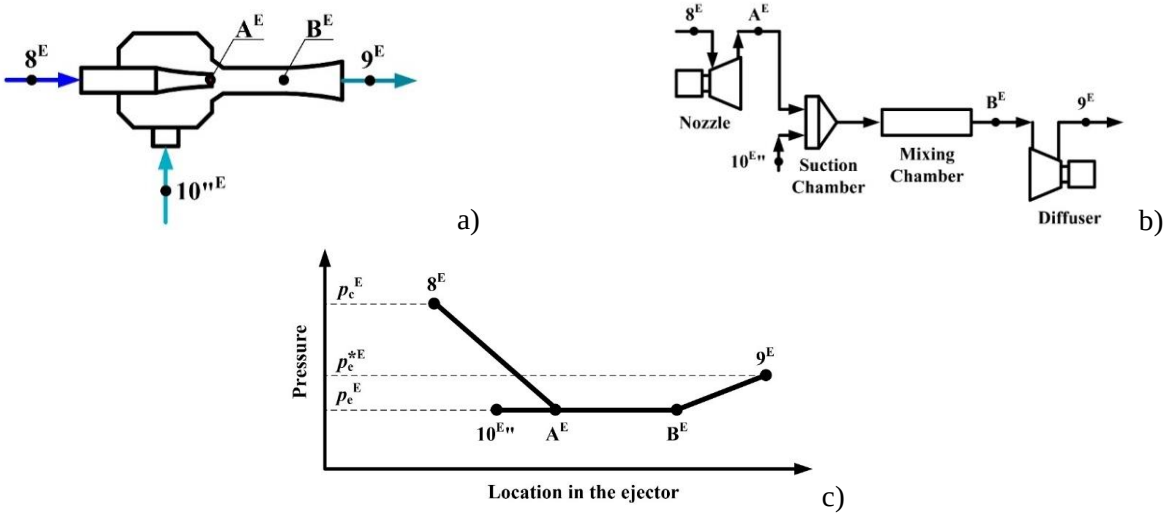

Figure 4 *– Schematic (a) and structural (b) diagram of the ejector, working processes in the ejector (c)*

To calculate the ejector parameters, it is necessary to set the initial value of the vapor quality at the diffuser outlet x_9^{E} and perform calculations by iteration with a sequential change in the value of this parameter [24]. The main calculated dependencies are presented in Eqs. (1)-(9).

The isentropic efficiency of the nozzle can be defined as:

$$\eta_{nozz} = \frac{h_{8^E} - h_{A^E}}{h_{8^E} - h_{A_s^E}}, \quad (1)$$

where h_8^{E} and h_A^{E} are the enthalpies of the working flow at the inlet and outlet of the nozzle; h_{As}^{E} is the specific enthalpy of the working flow at the outlet of the ideal nozzle (isentropic expansion).

To simplify calculations, the mixing pressure is assumed to equal the specified flow pressure: $p_{10}^{E"} = p_e^{E}$. Therefore, the value of h_{As}^{E} can be determined by the mixing pressure and the specific entropy under isentropic expansion $s_{As}^{E} = s_A^{E}$ by the equation of state. Neglecting the initial velocity of the working flow, the velocity of the working fluid flow at the ejector nozzle outlet is determined by applying the law of conservation of energy due to expansion:

$$\upsilon_{out}^{E} = \sqrt{2 \cdot \eta_{nozz} \cdot \left(h_{8^E} - h_{A_s^E}\right) \cdot 1000}. \quad (2)$$

On another side, the entrainment ratio ω can be determined with a known value of vapor quality x_9^{E} at the diffuser outlet. The refrigerant flow from the diffuser enters the bottoming stage separator in a state of wet vapor. After separation, the saturated vapor enters the compressor, and the saturated liquid passes through the expansion valve $EV1^{E}$ and is throttled to the pressure in the tank. The calculations assume that the mass of the working fluid at the ejector diffuser outlet is 1 kg. In this case, the expression for defining the entrainment ratio ω^{E} can be written as:

$$\omega^{E} = \frac{1 - x_{9^E}}{x_{9^E}}. \quad (3)$$

Eqs. (4) and (5) determine the mixing flow velocity υ_{B}^{E} and the specific enthalpy at the flow mixing site h_B^{E}:

$$\upsilon_{B^E} = \frac{\upsilon_{out} \cdot \sqrt{\eta_{mix}}}{1 + \omega}; \quad (4)$$

$$h_{B^E} = \frac{h_{8^E} + \omega^{E} \cdot h_{10^{E\prime\prime}}}{1 + \omega^{E}} - \frac{\upsilon_{B^E}^2}{2 \cdot 1000}. \quad (5)$$

Next, the specific entropy and temperature at the state B^{E} are determined:

$$s_{B^E}, t_{B^E} = f\left(p_e^{E}, h_{B^E}\right). \quad (6)$$

The specific enthalpy at the diffuser outlet is:

$$h_{9^E} = h_{B^E} + \frac{\upsilon_{B^E}^2}{2}. \quad (7)$$

For the isentropic operation conditions of the diffuser, the specific enthalpy at the diffuser outlet is determined by Eq. (8):

$$h_{9s^E} = h_{B^E} + \eta_{diff} \cdot \left(h_{9^E} - h_{B^E}\right). \quad (8)$$

The pressure at the diffuser outlet is:

$$p_{e^{*E}} = f\left(h_{9s^E}, s_{B^E}\right). \quad (9)$$

Next, the vapor quality at the diffuser outlet $x_{9\,calc}^{E}$ is determined. The calculation is performed by iteration method until the calculation error is:

$$\left| x_{9^E} - x_{9^E\,calc} \right| \le 0.005. \quad (10)$$

The parameters of the ejector outlet flow at the calculated values of the vapor quality for the bottoming and topping stages of the cascade are presented in Table 1. The properties of the working fluids were determined using the REFPROP software [25].

Table 1 *– Parameters of the ejector outlet flow*

Parameter	Value
Bottoming stage of the cascade (ethylene)	
Vapor quality x_9^{E}, kg·kg^{-1}	0.542
The velocity of the working fluid flow at the ejector nozzle outlet υ_{out}^{E}, m·s^{-1}	125.88
Entrainment ratio ω^{E}	0.844

Table 1 continuation

Parameter	Value
Mixing flow velocity v_B^E, m·s^{-1}	66.52
Specific enthalpy at the flow mixing site h_B^E, kJ·kg^{-1}	264.39
Specific entropy at the flow mixing site s_B^E, kJ·kg^{-1}·K^{-1}	1.548
Specific enthalpy at the diffuser outlet h_9^E, kJ·kg^{-1}	266.60
Specific enthalpy at the diffuser outlet at isentropic operation conditions h_{9s}^E, kJ·kg^{-1}	266.27
The calculated pressure at the diffuser outlet p_e^{*E}, bar	1.180
Topping stage of the cascade (propylene)	
Vapor quality x_9^R, kg·kg^{-1}	0.556
The velocity of the working fluid flow at the ejector nozzle outlet v_{out}^R, m·s^{-1}	131.03
Entrainment ratio ω^R	0.799
Mixing flow velocity v_B^R, m·s^{-1}	71.01
Specific enthalpy at the flow mixing site h_B^R, kJ·kg^{-1}	338.37
Specific entropy at the flow mixing site s_B^R, kJ·kg^{-1}·K^{-1}	1.663
Specific enthalpy at the diffuser outlet h_9^R, kJ·kg^{-1}	340.89
Specific enthalpy at the diffuser outlet at isentropic operation conditions h_{9s}^R, kJ·kg^{-1}	340.51
The calculated pressure at the diffuser outlet p_e^{*R}, bar	1.201

4.2. Energy analysis of the ERP system

Based on the ejector calculation data, the thermodynamic cycle of the ERP system was formed (Fig. 5) and an energy analysis of the cycle was performed by equations (11)-(16) and the information provided in [6, 26].

Bottoming cycle

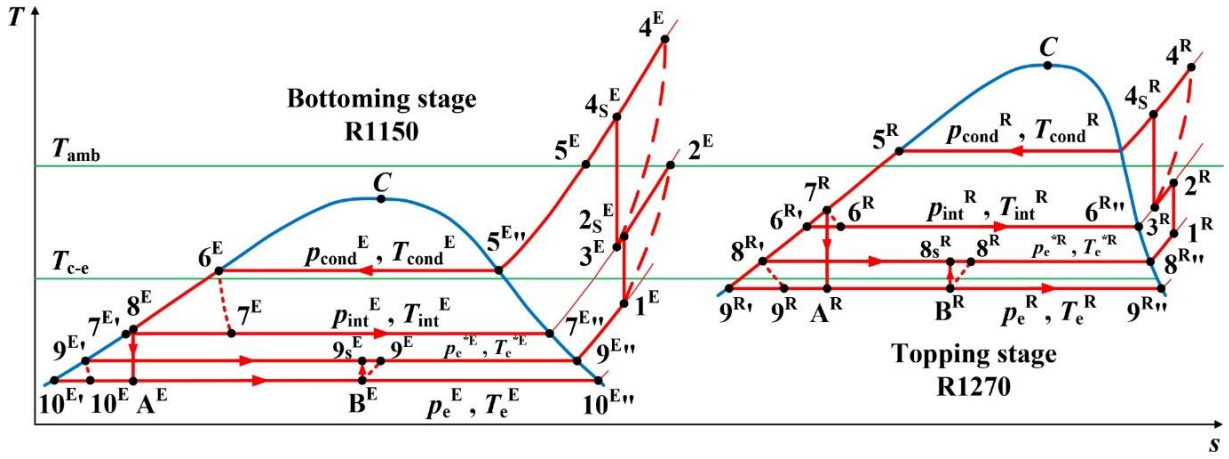

Figure 5 *– The thermodynamic cycle of the ERP system in the T-s diagram*

The entrainment ratio is:

$$\omega^E = \frac{\dot{m}_e^{LS}}{\dot{m}_e^{tank}}. \qquad (11)$$

The secondary mass flow rate of the ethylene is:

$$\dot{m}_e^{tank} = \frac{\dot{m}_e^{LS}}{\omega^E}. \qquad (12)$$

The mass flow rate of the ethylene at the diffuser outlet is:

$$\dot{m}_e^{tot} = \dot{m}_e^{tank} + \dot{m}_e^{LS}. \qquad (13)$$

Topping cycle

The entrainment ratio is:

$$\omega^R = \frac{\dot{m}_r^{c\text{-}e}}{\dot{m}_r^{LS}}. \qquad (14)$$

The secondary mass flow rate of the propylene is:

$$\dot{m}_r^{c\text{-}e} = \frac{m_e^{HS} \cdot \left(h_{5^{E''}} - h_{6^E}\right)}{\left(h_{9^{R''}} - h_{9^R}\right)}. \qquad (15)$$

The mass flow rate of the propylene in a high stage of the screw compressor is:

$$\dot{m}_{\mathrm{r}}^{\mathrm{HS}} = \frac{m_{\mathrm{r}}^{\mathrm{LS}} \cdot \left(h_{6^{\mathrm{R}}} - h_{6^{\mathrm{R}\prime\prime}}\right)}{\left(h_{5^{\mathrm{R}}} - h_{6^{\mathrm{R}\prime\prime}}\right)}. \qquad (16)$$

The results of the ERP system calculation and energy analysis are shown in Table 2.

***Table 2** – The results of the ERP system calculation and energy analysis*

Parameter	Value
Refrigeration capacity $\dot{Q}_{\mathrm{e}}$, kW	128.65
The mass flow rate of the ethylene in the low stage of the cargo reciprocating compressor $\dot{m}_{\mathrm{e}}^{\mathrm{LS}}$, kg·s^{-1}	0.269
The secondary mass flow rate of the ethylene $\dot{m}_{\mathrm{e}}^{\mathrm{tank}}$, kg·s^{-1}	0.318
The mass flow rate of the ethylene at the diffuser outlet $\dot{m}_{\mathrm{e}}^{\mathrm{tot}}$, kg·s^{-1}	0.587
The mass flow rate of the ethylene in the high stage of the cargo reciprocating compressor $\dot{m}_{\mathrm{e}}^{\mathrm{HS}}$, kg·s^{-1}	0.348
The secondary mass flow rate of the propylene $\dot{m}_{\mathrm{r}}^{\mathrm{c\text{-}e}}$, kg·s^{-1}	0.276
The mass flow rate of the propylene in a low stage of the screw compressor $\dot{m}_{\mathrm{r}}^{\mathrm{LS}}$, kg·s^{-1}	0.345
The mass flow rate of the propylene in a high stage of the screw compressor $\dot{m}_{\mathrm{r}}^{\mathrm{HS}}$, kg·s^{-1}	0.489
The mass flow rate of the ethylene through expansion valve EV2$^{\mathrm{E}}$ $\dot{m}_{\mathrm{e}}^{\mathrm{EV2}}$, kg·s^{-1}	0.079
The mass flow rate of the propylene through expansion valve EV2$^{\mathrm{R}}$ $\dot{m}_{\mathrm{r}}^{\mathrm{EV2}}$, kg·s^{-1}	0.144
Cargo reciprocating compressor power consumption $\dot{W}_{\mathrm{c,car}}$, kW	153.83
Screw compressor power consumption $\dot{W}_{\mathrm{c,scr}}$, kW	91.56
Coefficient of performance *COP*	0.53
Condensing heat load $\dot{Q}_{\mathrm{cond}}$, kW	229.68
The heat load at the condenser-evaporator $\dot{Q}_{\mathrm{c\text{-}e}}$, kW	119.42
The heat load at the LPG heat exchanger $\dot{Q}_{\mathrm{LPG}}$, kW	32.80
The heat load at the economizer $\dot{Q}_{\mathrm{ec}}$, kW	54.77
The heat load at the precooler $\dot{Q}_{\mathrm{pc}}$, kW	41.21

5. The method of the ERP system performance evaluation

The performance evaluation is based on the results of the exergy analysis of the ERP system, as it is recognized as a reliable method for the energy efficiency engineering evaluation of the energy systems. The concept and methodology of used exergy analysis are described in [27-29].

The total exergy balance can be expressed as:

$$\dot{E}_{\dot{\mathrm{Q}}} + \dot{W} = \sum \dot{E}_{\mathrm{i}}^{\mathrm{in}} - \sum \dot{E}_{\mathrm{i}}^{\mathrm{out}} + \Delta \dot{E}_{\mathrm{i}}, \qquad (17)$$

where $\dot{\mathrm{E}}_{\mathrm{Q}}$ is the exergy of heat at temperature T:

$$\dot{E}_{\dot{\mathrm{Q}}} = \dot{Q} \cdot \left(\frac{1 - T_{\mathrm{amb}}}{T}\right). \qquad (18)$$

$\dot{E}_{\mathrm{i}}^{\mathrm{in}}$ and $\dot{E}_{\mathrm{i}}^{\mathrm{out}}$ are incoming and outgoing flows of physical exergy for the i-th component; $\Delta \dot{E}_{\mathrm{i}}$ is the exergy loss associated with the irreversibility of processes in the system.

The physical exergy for the i-th component is determined by Eq. (19):

$$\dot{E}_{\mathrm{i}} = \dot{m}_{\mathrm{i}} \cdot e_{\mathrm{i}}, \qquad (19)$$

where e_{i} is the specific physical exergy of the flow resulting from temperature and pressure differences:

$$e_{\mathrm{i}} = h_{\mathrm{i}} - h_{\mathrm{amb}} - T_{\mathrm{amb}} \cdot \left(s_{\mathrm{i}} - s_{\mathrm{amb}}\right). \qquad (20)$$

The efficient operation of the ethylene reliquefaction system is achieved by minimizing any type of exergy loss. Exergy loss is quantified and thermodynamically related to entropy production by the Gouy-Stodola equation:

$$\Delta \dot{E}_{\mathrm{i}} = T_{\mathrm{amb}} \cdot \Delta s_{\mathrm{tot}}, \qquad (21)$$

where Δs_{tot} is the entropy generation in the process.

Total exergy loss $\Delta \dot{E}_{\mathrm{tot}}$ represents the sum of the individual exergy losses in these components:

$$\Delta \dot{E}_{\mathrm{tot}} = \sum_{\mathrm{i}=1}^{\mathrm{n}} \Delta \dot{E}_{\mathrm{i}} \qquad (22)$$

The exergy of ethylene reliquefaction $\dot{\mathrm{E}}_{\mathrm{LEG}}$ is determined by the expression:

$$\dot{E}_{\mathrm{LEG}} = \dot{m}_{\mathrm{LEG}} \cdot e_{\mathrm{LEG}} \qquad (23)$$

The exergy efficiency of the ERP system is defined as:

$$\varepsilon = 1 - \frac{\Delta \dot{E}_{\text{tot}}}{\sum \dot{W}_{\text{ad}}} \quad (24)$$

The performance improvement of the ERP system is evaluated in terms of energy efficiency COP and exergy efficiency ε:

$$\gamma_{\text{COP}} = \frac{COP_{\text{ERP}} - COP_{\text{CRP}}}{COP_{\text{CRP}}} \cdot 100\% \quad (25)$$

$$\gamma_{\varepsilon} = \frac{\varepsilon_{\text{ERP}} - \varepsilon_{\text{CRP}}}{\varepsilon_{\text{CRP}}} \cdot 100\% \quad (26)$$

The exergy analysis of the ERP system components was performed according to Eqs. (27)-(45) presented in Tables 3 and 4:

Table 3 *– The exergy analysis of the ERP system components (bottoming cycle)*

Bottoming cycle of the cascade (ethylene)		
Component		**Equation**
Cargo reciprocating compressor (low stage)	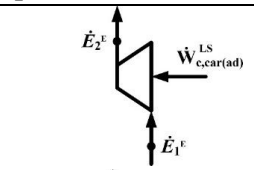	$\Delta \dot{E}^{\text{LS}}_{\text{c,car}} = \dot{m}^{\text{LS}}_{\text{e}} \cdot \left(e_{\text{e1}} - e_{\text{e2}}\right) + \dot{W}^{\text{LS}}_{\text{c,car(ad)}}$, kW (27)
Cargo reciprocating compressor (high stage)	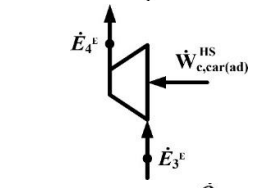	$\Delta \dot{E}^{\text{HS}}_{\text{c,car}} = \dot{m}^{\text{HS}}_{\text{e}} \cdot \left(e_{\text{e3}} - e_{\text{e4}}\right) + \dot{W}^{\text{HS}}_{\text{c,car(ad)}}$, kW (28)
LPG heat exchanger	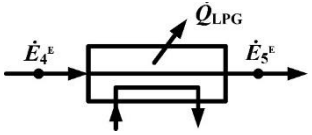	$\Delta \dot{E}_{\text{LPG}} = \dot{m}^{\text{HS}}_{\text{e}} \cdot \left(e_{\text{e4}} - e_{\text{e5}}\right)$, kW (29)
Precooler		$\Delta \dot{E}_{\text{pc}} = \dot{m}^{\text{HS}}_{\text{e}} \cdot \left(e_{\text{e5}} - e_{\text{e5''}}\right) + \dot{m}^{\text{LS}}_{\text{r}} \cdot \left(e_{\text{r8''}} - e_{\text{r1}}\right)$, kW (30)
Condenser-evaporator		$\Delta \dot{E}_{\text{c-e}} = \dot{m}^{\text{HS}}_{\text{e}} \cdot \left(e_{\text{e5''}} - e_{\text{e6}}\right) + \dot{m}^{\text{c-e}}_{\text{r}} \cdot \left(e_{\text{r9}} - e_{\text{r9''}}\right)$, kW (31)
Intermediate vessel	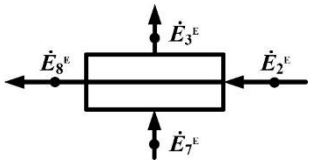	$\Delta \dot{E}_{\text{int}} = \dot{m}^{\text{LS}}_{\text{e}} \cdot \left(e_{\text{e2}} - e_{\text{e8}}\right) + \dot{m}^{\text{HS}}_{\text{e}} \cdot \left(e_{\text{e7}} - e_{\text{e3}}\right)$, kW (32)
Expansion valve $EV1^{E}$		$\Delta \dot{E}_{\text{EV1}^{\text{E}}} = \dot{m}^{\text{tank}}_{\text{e}} \cdot \left(e_{\text{e9'}} - e_{\text{e10}}\right)$, kW (33)
Expansion valve $EV2^{E}$		$\Delta \dot{E}_{\text{EV2}^{\text{E}}} = \dot{m}^{\text{EV2}}_{\text{e}} \cdot \left(e_{\text{e6}} - e_{\text{e7}}\right)$, kW (34)
Bottoming stage ejector	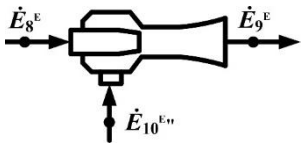	$\Delta \dot{E}_{\text{ej}^{\text{E}}} = \dot{m}^{\text{LS}}_{\text{e}} \cdot e_{\text{e8}} - \left(\dot{m}^{\text{LS}}_{\text{e}} + \dot{m}^{\text{tank}}_{\text{e}}\right) \cdot e_{\text{e9}} + \dot{m}^{\text{tank}}_{\text{e}} \cdot e_{\text{e10''}}$, kW (35)

Table 3 continuation

Component	Equation
Bottoming stage separator 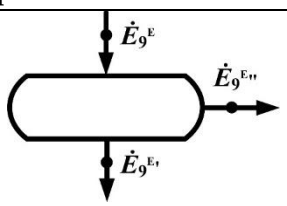	$\Delta\dot{E}_{\text{sep}^{\text{E}}} = \left(\dot{m}_{\text{e}}^{\text{LS}} + \dot{m}_{\text{e}}^{\text{tank}}\right)\cdot e_{\text{e9}} - \dot{m}_{\text{e}}^{\text{LS}}\cdot e_{\text{e9}''} - \dot{m}_{\text{e}}^{\text{tank}}\cdot e_{\text{e9}'}$, kW (36)
Tank 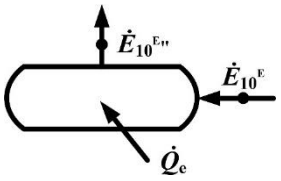	$\Delta\dot{E}_{\text{tank}} = \dot{m}_{\text{e}}^{\text{tank}}\cdot\left(e_{\text{e10}'} - e_{\text{e10}''}\right) + \left(1 - \frac{T_{\text{amb}}}{T_{\text{LEG}}}\right)$, kW (37)

Table 4 *– The exergy analysis of the ERP system components (topping cycle)*

Topping cycle of the cascade (propylene)	
Component	**Equation**
Screw compressor (low stage) 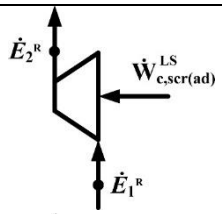	$\Delta\dot{E}_{\text{c,scr}}^{\text{LS}} = \dot{m}_{\text{r}}^{\text{LS}}\cdot\left(e_{\text{r1}} - e_{\text{r2}}\right) + \dot{W}_{\text{c,scr(ad)}}^{\text{LS}}$, kW (38)
Screw compressor (high stage) 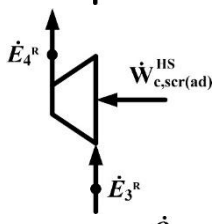	$\Delta\dot{E}_{\text{c,scr}}^{\text{HS}} = \dot{m}_{\text{r}}^{\text{HS}}\cdot\left(e_{\text{r3}} - e_{\text{r4}}\right) + \dot{W}_{\text{c,scr(ad)}}^{\text{HS}}$, kW (39)
Condenser 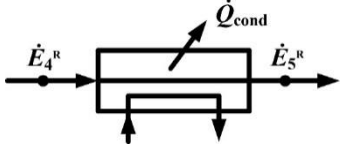	$\Delta\dot{E}_{\text{cond}} = \dot{m}_{\text{r}}^{\text{HS}}\cdot\left(e_{\text{r4}} - e_{\text{r5}}\right)$, kW (40)
Economizer 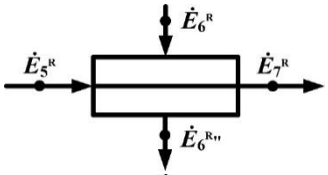	$\Delta\dot{E}_{\text{ec}} = \dot{m}_{\text{r}}^{\text{HS}}\cdot\left(e_{\text{e5}} - e_{\text{e7}}\right) + \dot{m}_{\text{r}}^{\text{EV2}}\cdot\left(e_{\text{r6}} - e_{\text{r6}''}\right)$, kW (41)
Expansion valve $EV1^{R}$ 	$\Delta\dot{E}_{\text{EV1}^{\text{R}}} = \dot{m}_{\text{r}}^{\text{c-e}}\cdot\left(e_{\text{r8}'} - e_{\text{r9}}\right)$, kW (42)
Expansion valve $EV2^{R}$ 	$\Delta\dot{E}_{\text{EV2}^{\text{R}}} = \dot{m}_{\text{r}}^{\text{EV2}}\cdot\left(e_{\text{r7}} - e_{\text{r6}}\right)$, kW (43)
Topping stage ejector 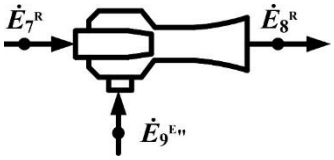	$\Delta\dot{E}_{\text{ej}^{\text{R}}} = \dot{m}_{\text{r}}^{\text{LS}}\cdot e_{\text{r7}} - \left(\dot{m}_{\text{r}}^{\text{LS}} + \dot{m}_{\text{r}}^{\text{c-e}}\right)\cdot e_{\text{r8}} + \dot{m}_{\text{r}}^{\text{c-e}}\cdot e_{\text{r9}''}$, kW (44)
Topping stage separator 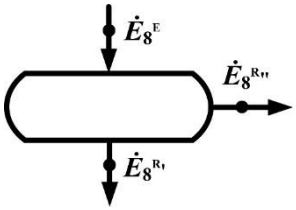	$\Delta\dot{E}_{\text{sep}^{\text{R}}} = \left(\dot{m}_{\text{r}}^{\text{LS}} + \dot{m}_{\text{r}}^{\text{c-e}}\right)\cdot e_{\text{r8}} - \dot{m}_{7}^{\text{LS}}\cdot e_{\text{r8}''} - \dot{m}_{\text{r}}^{\text{c-e}}\cdot e_{\text{e8}'}$, kW (45)

The exergy analysis of the components of the CRP system is performed similarly. The calculated results of CRM and ERP systems considering specific exergy parameters of material flows and mass costs for the system components are presented in Table 5.

Table 5 *– The results of the ERP and CRP system exergy analysis*

Parameter	Value	
	CRP system	**ERP system**
The exergy loss in the low stage of the cargo reciprocating compressor $\Delta\dot{E}_{c,car}^{LS}$, kW	20.10	20.37
The exergy loss in the high stage of the cargo reciprocating compressor $\Delta\dot{E}_{c,car}^{HS}$, kW	5.17	3.66
The exergy loss in the LPG heat exchanger $\Delta\dot{E}_{LPG}$, kW	3.76	5.47
The exergy loss in the precooler $\Delta\dot{E}_{pc}$, kW	-	1.91
The exergy loss in the condenser-evaporator $\Delta\dot{E}_{c\text{-}e}$, kW	14.16	7.05
The exergy loss in the intermediate vessel $\Delta\dot{E}_{int}$, kW	7.59	2.33
The exergy loss in the expansion valve EV1^{E} $\Delta\dot{E}_{EV1}^{E}$, kW	3.97	~0
The exergy loss in the expansion valve EV2^{E} $\Delta\dot{E}_{EV2}^{E}$, kW	1.25	1.29
The exergy loss in the bottoming stage ejector $\Delta\dot{E}_{ej}^{E}$, kW	-	2.50
The exergy loss in the bottoming stage separator $\Delta\dot{E}_{sep}^{E}$, kW	-	0.20
The exergy loss in the tank $\Delta\dot{E}_{tank}$, kW	0.08	0.01
The exergy loss in the low stage of the screw compressor $\Delta\dot{E}_{c,scr}^{LS}$, kW	0	0
The exergy loss in the high stage of the screw compressor $\Delta\dot{E}_{c,scr}^{HS}$, kW	5.33	4.48
The exergy loss in the condenser $\Delta\dot{E}_{cond}$, kW	12.70	18.43
The exergy loss in the economizer $\Delta\dot{E}_{ec}$, kW	6.59	2.44
The exergy loss in the expansion valve EV1^{R} $\Delta\dot{E}_{EV1}^{R}$, kW	5.75	~0
The exergy loss in the expansion valve EV2^{R} $\Delta\dot{E}_{EV2}^{R}$, kW	0.41	0.33
The exergy loss in the topping stage ejector $\Delta\dot{E}_{ej}^{R}$, kW	-	2.44
The exergy loss in the topping stage separator $\Delta\dot{E}_{sep}^{R}$, kW	-	0.01
The total exergy loss in the system $\Delta\dot{E}_{tot}$, kW	86.87	73.00
The exergy efficiency of the system ε	0.48	0.56

6. Discussion of the results and conclusions

The paper presents the cycle analysis for the actual CRP system and the proposed ERP system from an energy and exergy efficiency point of view. Figs. 6 and 7 illustrate the ratio of exergy losses relative to the total exergy of the installation for each cycle.

In both cycles, the cargo reciprocating compressor has the highest exergetic loss (29.0 and 34.1% for he CRP and ERP cycles, respectively). For the CRP cycle, the highest exergy loss is observed in the condenser-evaporator (16.3%).

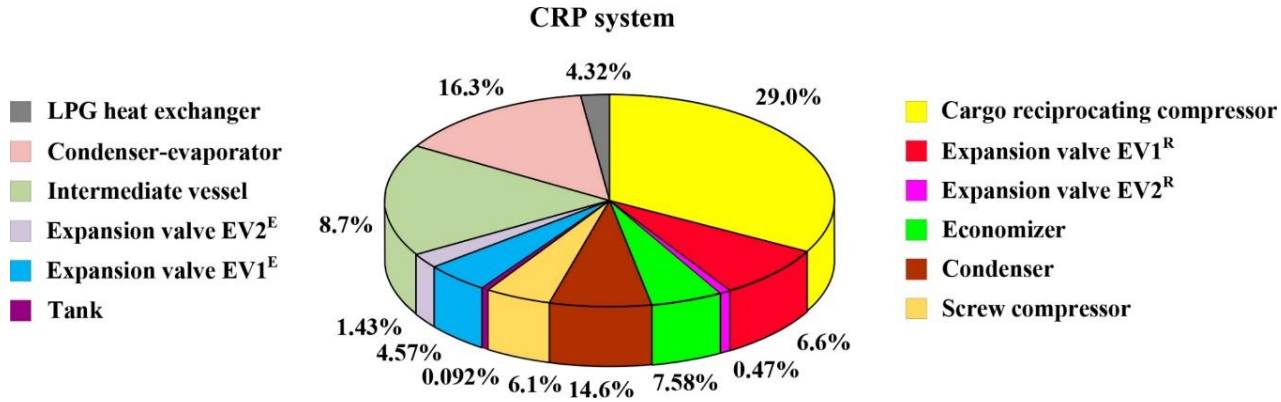

Figure 6 *– Distribution of exergy losses in the CRP system*

In the ERP cycle, the condenser is the most imperfect (26.0%). The total exergy loss in the expansion devices of the CRP cycle is 13.07%, and the total exergy loss in the expansion devices of the ERP cycle is 9.34%. Exergy loss in the intermediate vessel is 8.7% (the CRP cycle) and 3.31% (the ERP cycle).

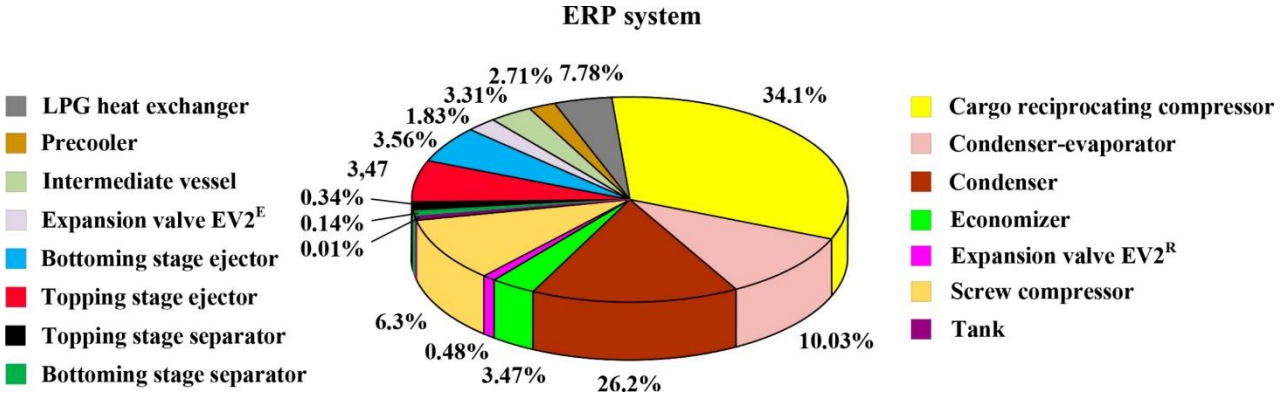

Figure 7 *– Distribution of exergy losses in the ERP system*

Fig. 8 shows the absolute values of exergy losses in the components of the CRM and ERP systems. The exergy losses in each component of the ERP system are lower than the corresponding values in the CRP system component. The exception is exergy losses in the condenser and precooler. Replacement of throttle devices led to a decrease in exergetic losses from 9.75 to 4.95 kW. Calculations have shown an increase in the energy efficiency of the ERP system (COP) by 24.0% and the exergetic efficiency (ε) by 16.0%.

Based on the results of calculations, it was concluded that the proposed ERP system meets IMO requirements regarding vessel energy efficiency. But it should be considered that the ejector is calculated for only one mode. Any deviations from the calculated values lead to a violation of the operating parameters of the entire installation.

The operation of reliquefaction installation depends on external factors (roll, deflector, outdoor air temperature, seawater temperature, etc.) and therefore requires reliable methods of regulating productivity. For actual installations with ejectors, the performance-adjusting way can be technically complicated.

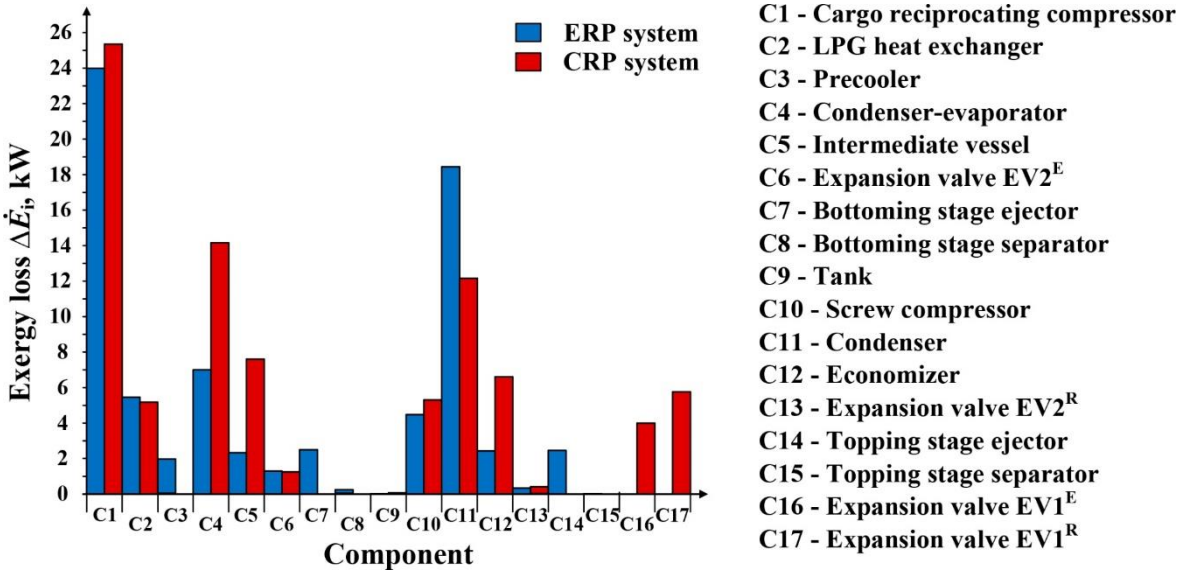

Figure 8 *– Exergy losses in components of CRM and ERP systems*

CRediT author statement

Larisa Morosuk: Conceptualization, Formal analysis, Writing – Review & Editing. **Victoriia Sokolovska-Yefymenko**: Methodology, Writing – Original Draft, Project administration, Supervision. **Volodymyr Ierin**: Investigation, Data Curation, Writing – Review & Editing. **Oleksandr Yefymenko**: Funding acquisition, Resources, Software. **Andrii Moshkatiuk**: Visualization, Validation.

References

1. **Lee, D.-H., Ha, M.-K., Kim, S.-Y., Shin, S.-C.** (2014) Research of design challenges and new technologies for floating LNG. *International Journal of Naval Architecture and Ocean Engineering, 6, 307-322.* https://doi.org/10.2478/IJNAOE-2013-0181.

2. **Yazır, D., Şahin, B., Yip, T.L.** (2021) Selection of new design gas carriers by using fuzzy EVAMIX method. *The Asian Journal of Shipping and Logistics, 37, 91-104.* https://doi.org/10.1016/j.ajsl.2020.10.001.

3. Annex VI of MARPOL 73/78-Regulations for the Prevention of Air Pollution from Ships. Retrived 26 January 2023 from https://www.maritimenz.govt.nz/rules/MARPOL-Annex-VI/default.asp.

4. **Li, Y., Jin, G., Zhong, Z.** (2012) Thermodynamic Analysis-Based Improvement for the Boil-off Gas Reliquefaction Process of Liquefied Ethylene Vessels. *Chemical Engineering & Technology, 35.* https://doi.org/10.1002/ceat.201200019.

5. **Ouadha, A., Beladjine, B.** (2015) Exergy analysis of an ethylene BOG re-liquefaction system. *Proceedings of the 24th IIR International Congress of Refrigeration, August 16-22, Yokohama, Japan, ID 553.* http://dx.doi.org/10.18462/iir.icr.2015.0553.

6. **Sokolovska-Yefymenko, V., Morozyuk, L., Ierin, V., Yefymenko, O.** (2023). Thermodynamic Analysis of an Ethylene Reliquefaction System Using the Entropy-Cycle Method. *Energies 16, 920*. https://doi.org/10.3390/en16020920.

7. **Tan, H., Sun, N., Zhao, Q., Li, Y.** (2017) An ejector-enhanced re-liquefaction process (EERP) for liquid ethylene vessels. *International Journal of Energy Research, 41, 658-672.* https://doi.org/10.1002/er.3658

8. **Tan, H., Zhang, Y., Shan, S., Zhao, Q.** (2019) Comparative study of boil-off gas re-liquefaction processes for liquid ethylene vessels. *Journal of Marine Science and Technology 24, 209-220.* https://doi.org/10.1007/s00773-018-0547-1.

9**. Berlinck, E.C., Parise, J.A.R., Pitanga Marques, R.** (1997) Numerical simulation of an ethylene re-liquefaction plant. *International Journal of Energy Research,* 21, 597-614. https://doi.org/10.1002/(SICI)1099-114X(19970610)21:7<597::AID-ER193>3.0.CO;2-5.

10. **Chien, M.D., Shih, M.-Y.** (2011) An Innovative Optimization Design for a Boil-off Gas Reliquefaction Process of LEG Vessels. *Journal of Petroleum Science and Engineering, 47(4), 65-74.*

11. **Nanowski, D.** (2016) The influence of incondensible gases on the refrigeration capacity of the reliquefaction plant during ethylene carriage by sea. *Journal of KONES Powertrain and Transport 23, 359-364.* https://kones.eu/ep/2016/vol23/no3/359-364_J_O_KONES_2016_NO._3_VOL._23_ISSN_1231-4005_NANOWSKI.pdf.

12. **Tan, H., Cai, W., Wang, Q.-g., Sun, N.** (2016) Optimization and comparison of boiling-off gas reliquefaction processes for liquid ethylene vessels. *2016 IEEE 11th Conference on Industrial Electronics and Applications (ICIEA), 5-7 June, Hefei, China, 717-722.* https://doi.org/10.1109/ICIEA.2016.7603676

13**. Sarkar, J.** (2012) Ejector enhanced vapor compression refrigeration and heat pump systems — A review. *Renewable and Sustainable Energy Reviews, 16, 6647-6659.* https://doi.org/10.1016/j.rser.2012.08.007.

14. **Sumeru, K., Nasution, H., Ani, F.N.** (2012) A review on two-phase ejector as an expansion device in vapor compression refrigeration cycle. *Renewable and Sustainable Energy Reviews, 16, 4927-4937*. https://doi.org/10.1016/j.rser.2012.04.058.

15. **Chen, J., Jarall, S., Havtun, H., Palm, B.** (2015) A review on versatile ejector applications in refrigeration systems. *Renewable and Sustainable Energy Reviews, 49, 67-90.* https://doi.org/10.1016/j.rser.2015.04.073

16. **Mondal, S., De, S.** (2020) Performance assessment of a low-grade heat driven dual ejector vapour compression refrigeration cycle. *Applied Thermal Engineering, 179, 115782.* https://doi.org/10.1016/j.applthermaleng.2020.115782.

17. **Wongwises, S., Disawas, S.** (2005) Performance of the two-phase ejector expansion refrigeration cycle. *International Journal of Heat and Mass Transfer, 48, 4282-4286.* https://doi.org/10.1016/j.ijheatmasstransfer.2005.04.017.

18. **Ma, M., Yu, J., Wang, X.** (2014) Performance evaluation and optimal configuration analysis of a CO2/NH3 cascade refrigeration system with falling film evaporator–condenser. *Energy Conversion and Management, 79, 224-231.* https://doi.org/10.1016/j.enconman.2013.12.021.

19. **Dopazo, J.A., Fernández-Seara, J., Sieres, J., Uhía, F.J.** (2009) Theoretical analysis of a CO2–NH3 cascade refrigeration system for cooling applications at low temperatures. *Applied Thermal Engineering, 29, 1577-1583.* https://doi.org/10.1016/j.applthermaleng.2008.07.006.

20. **Yari, M., Sirousazar, M.** (2008) Cycle improvements to ejector-expansion transcritical CO2 two-stage refrigeration cycle. *International Journal of Energy Research, 32, 677-687*. https://doi.org/10.1002/er.1385.

21. **Li, D., Groll, E.A.** (2005) Transcritical CO2 refrigeration cycle with ejector-expansion device. *Inter-*

national Journal of Refrigeration, 28, 766-773. https://doi.org/10.1016/j.ijrefrig.2004.10.008.
22. VesselFinder. ANTIKITHIRA, LPG Tanker, IMO 9788980. Retrived 26 January 2023 from https://www.vesselfinder.com/vessels/ANTIKITHIRA-IMO-9788980-MMSI-636020291.
23. **Yu, J., Zhao, H., Li, Y.** (2008) Application of an ejector in autocascade refrigeration cycle for the performance improvement. *International Journal of Refrigeration, 31, 279-286.* https://doi.org/10.1016/j.ijrefrig.2007.05.008.
24. **Yu, J., Ren, Y., Chen, H., Li, Y.** (2007) Applying mechanical subcooling to ejector refrigeration cycle for improving the coefficient of performance. *Energy Conversion and Management, 48, 1193-1199.* https://doi.org/10.1016/j.enconman.2006.10.009.
25. **Lemmon, E.W., Bell, I.H., Huber, M.L., McLinden, M.O.** (2018) Reference fluid thermodynamic and transport properties database (REFPROP), Version 10.0; NIST Standard Reference Database 23; *National Institute of Standards and Technology: Gaithersburg, MD, USA.*
26. **Morosuk, L.** (2016) Cascade refrigeration machines with R744 as the working fluid for the high-temperature cascade. *Refrigeration Engineering and Technology, 52, 12-17.* https://doi.org/10.21691/ret.v52i1.32.
27. **Brodyansky, V.M., Sorin, M.V., Goff, P.L.** (1994) The Efficiency of Industrial Processes: Exergy Analysis and Optimization. *Elsevier Inc, 487.*
28. **Moran, M.J., Shapiro, H.N.** (2014) Fundamentals of Engineering Thermodynamics. 4th ed. *John Wiley & Sons: New York, 932.*
29. **Kotas, T.J.** (1985) The Exergy Method of Thermal Plant Analysis. *London, Butterworth-Heinemann, 320*. https://doi.org/10.1016/C2013-0-00894-8.

Received 09 February 2023
Approved 16 March 2023
Available in Internet 31 March 2023

Термодинамічний аналіз системи повторного зрідження етилену на LEG газовозах при заміні дросельних пристроїв на ежектори

Л.І. Морозюк[1], В.В. Соколовська-Єфименко[2]✉, В.О. Єрін[3], О.О. Єфименко[4], А.В. Мошкатюк[5]
[1,2,4,5]Одеський національний технологічний університет, вул. Канатна, 112, Одеса, 65039, Україна;
[3]Технологічний університет Нінбо, 1 Qian Hu South Road, Нінбо, 315100, Китай
✉ e-mail: [2]kli24062006@gmail.com
ORCID: [1]http://orcid.org/0000-0003-4133-1984; [2]http://orcid.org/0000-0002-7275-5061; [3]http://orcid.org/0000-0001-7941-9725; [4]http://orcid.org/0000-0003-2571-9292; [5]http://orcid.org/0000-0003-3354-0321

Підвищення енергетичної ефективності суден-газовозів типу LEG, може бути досягнуто шляхом удосконалення процесів установки повторного зрідження відпарного газу (BOG) в окремих її елементах. У цьому дослідженні пропонується замінити звичайний процес повторного зрідження (CRP) дійсної установки на LEG танкері «ANTIKITIRA» з дросельними пристроями на ежекторний процес повторного зрідження (ERP) з двофазними ежекторами у якості розширювальних пристроїв для підвищенням енергетичної ефективності установки. В запропонованій схемі дросельні пристрої ($EV2^E$ і $EV2^R$) було змінено на двофазні ежектори. Працездатність ежекторів забезпечено встановленням додаткового обладнання: сепараторів та попереднього охолоджувача в нижньому каскаді. Сепаратори підтримують постійний тиск на входах в компресори, а попередній охолоджувач зменшує навантаження на конденсатор-випарник. Розроблено модель ежектора для аналізу запропонованої системи. На підставі багатоваріантних розрахунків визначено розрахунковий тиск на виході із сопла ежектора. Проведено енергетичні та ексергетичні аналізи установки ERP та установки CRP. За результатами ексергетичного аналізу оцінено вплив кожного компонента на енергетичну ефективність систем CRP та ERP. Втрати ексергії у кожному компоненті ERP нижчі, ніж відповідні значення у компонентах CRP. Втрати в конденсаторі та попередньому охолоджувачі у компонентах CRP нижчі, ніж у ERP. Загальна споживана потужність однакова в обох циклах, а холодопродуктивність циклу ERP збільшилася на 29,1 кВт. Заміна розширювальних пристроїв призвела до зниження абсолютних ексергетичних втрат із 9,75 до 4,95 кВт. Енергетична ефективність ERP циклу збільшилася на 24%, а ексергетична ефективність збільшилася на 16%. Найбільші втрати ексергії в обох циклах спостерігаються у процесі

стиснення в двоступеневому вантажному компресорі нижнього каскаду (29,0-34,1%). Зроблено висновок, що запропонований цикл ERP відповідає вимогам IMO щодо енергоефективності суден, але вимагає додаткових капітальних вкладень.

Ключові слова: *Етилен; Ежектор; Ексергетичний аналіз; Установка повторного зрідження*

Література

1. **Lee D.-H., Ha M.-K., Kim S.-Y., Shin S.-C.** Research of design challenges and new technologies for floating LNG // International Journal of Naval Architecture and Ocean Engineering. – 2014. – Vol. 6. – P. 307-322.

2. **Yazır D., Şahin B., Yip T.L.** (2021) Selection of new design gas carriers by using fuzzy EVAMIX method // The Asian Journal of Shipping and Logistics. – 2021. – Vol. 37. – P. 91-104.

3. Annex VI of MARPOL 73/78-Regulations for the Prevention of Air Pollution from Ships. URL: https://www.maritimenz.govt.nz/rules/MARPOL-Annex-VI/default.asp (дата звернення: 26.01.2023).

4. **Li Y., Jin G., Zhong Z.** Thermodynamic Analysis-Based Improvement for the Boil-off Gas Reliquefaction Process of Liquefied Ethylene Vessels // Chemical Engineering & Technology. – 2012. – Vol. 35.

5. **Ouadha A., Beladjine B.** Exergy analysis of an ethylene BOG re-liquefaction system // Proceedings of the 24th IIR International Congress of Refrigeration. – August 16-22, 2015, Yokohama, Japan. – ID 553.

6. **Sokolovska-Yefymenko V., Morozyuk L., Ierin V., Yefymenko O.** (2023). Thermodynamic Analysis of an Ethylene Reliquefaction System Using the Entropy-Cycle Method. Energies 16, 920. https://doi.org/10.3390/en16020920

7. **Tan H., Sun N., Zhao Q., Li Y.** An ejector-enhanced re-liquefaction process (EERP) for liquid ethylene vessels // International Journal of Energy Research. – 2017. – Vol. 41. – P. 658-672.

8. **Tan H., Zhang Y., Shan S., Zhao Q.** Comparative study of boil-off gas re-liquefaction processes for liquid ethylene vessels // Journal of Marine Science and Technology. – 2019. – Vol. 24. – P. 209-220.

9**. Berlinck E.C., Parise J.A.R., Pitanga Marques R.** Numerical simulation of an ethylene re-liquefaction plant // International Journal of Energy Research. – 1997. – Vol. 21. – P. 597-614.

10. **Chien M.D., Shih M.-Y.** An Innovative Optimization Design for a Boil-off Gas Reliquefaction Process of LEG Vessels // Journal of Petroleum Science and Engineering. – 2011. – Vol. 47(4). – P. 65-74.

11. **Nanowski D.** The influence of incondensible gases on the refrigeration capacity of the reliquefaction plant during ethylene carriage by sea // Journal of KONES Powertrain and Transport. – 2016. – Vol. 23. – P. 359-364.

12. **Tan H., Cai W., Wang Q.-g., Sun N.** Optimization and comparison of boiling-off gas re-liquefaction processes for liquid ethylene vessels // 2016 IEEE 11th Conference on Industrial Electronics and Applications (ICIEA). – 5-7 June, 2016, Hefei, China. – P. 717-722.

13**. Sarkar J.** Ejector enhanced vapor compression refrigeration and heat pump systems — A review // Renewable and Sustainable Energy Reviews. – 2012. – Vol. 16. – P. 6647-6659.

14. **Sumeru K., Nasution H., Ani F.N.** A review on two-phase ejector as an expansion device in vapor compression refrigeration cycle // Renewable and Sustainable Energy Reviews. – 2012. – Vol. 16. – P. 4927-4937.

15. **Chen J., Jarall S., Havtun H., Palm B.** A review on versatile ejector applications in refrigeration systems // Renewable and Sustainable Energy Reviews. – 2015. – Vol. 49. – P. 67-90.

16. **Mondal S., De S.** Performance assessment of a low-grade heat driven dual ejector vapour compression refrigeration cycle // Applied Thermal Engineering. – 2020. – Vol. 179. – P. 115782.

17. **Wongwises, S., Disawas, S.** Performance of the two-phase ejector expansion refrigeration cycle // International Journal of Heat and Mass Transfer. – 2005. – Vol. 48. – P. 4282-4286.

18. **Ma M., Yu J., Wang X.** Performance evaluation and optimal configuration analysis of a CO2/NH3 cascade refrigeration system with falling film evaporator–condenser // Energy Conversion and Management. – 2014. – Vol. 79. – P. 224-231.

19. **Dopazo J.A., Fernández-Seara J., Sieres J., Uhía F.J.** Theoretical analysis of a CO2–NH3 cascade refrigeration system for cooling applications at low temperatures // Applied Thermal Engineering. – 2009. – Vol. 29. – P. 1577-1583.

20. **Yari M., Sirousazar M.** Cycle improvements to ejector-expansion transcritical CO2 two-stage refrigeration cycle // International Journal of Energy Research. – 2008. – Vol. 32. – P. 677-687.

21. **Li D., Groll E.A.** Transcritical CO2 refrigeration cycle with ejector-expansion device // International

Journal of Refrigeration. – 2005. – Vol. 28. – P. 766-773.
22. VesselFinder. ANTIKITHIRA, LPG Tanker, IMO 9788980. URL: https://www.vesselfinder.com/vessels/ANTIKITHIRA-IMO-9788980-MMSI-636020291 (дата звернення: 26.01.2023).
23. **Yu J., Zhao H., Li Y.** Application of an ejector in autocascade refrigeration cycle for the performance improvement // International Journal of Refrigeration. – 2008. – Vol. 31. – P. 279-286.
24. **Yu J., Ren Y., Chen H., Li Y.** Applying mechanical subcooling to ejector refrigeration cycle for improving the coefficient of performance // Energy Conversion and Management. – 2007. – Vol. 48. – P. 1193-1199.
25. **Lemmon E.W., Bell I.H.; Huber M.L., McLinden M.O.** Reference fluid thermodynamic and transport properties database (REFPROP), Version 10.0; NIST Standard Reference Database 23 // National Institute of Standards and Technology: Gaithersburg, MD, USA. – 2018.
26. **Морозюк Л.І.** Термодинамічний аналіз каскадних холодильних машин з R744 у верхньому каскаді // Холодильна техніка та технологія. – 2016. – Т. 52. – С. 12-17.
27. **Brodyansky, V.M., Sorin, M.V., Goff, P.L.** The Efficiency of Industrial Processes: Exergy Analysis and Optimization. – Elsevier Inc, 1994. – 487 p.
28. **Moran, M.J., Shapiro, H.N.** Fundamentals of Engineering Thermodynamics. 4th ed. – John Wiley & Sons: New York, 2014. – 932 p.
29. **Kotas, T.J.** The Exergy Method of Thermal Plant Analysis. – London: Butterworth-Heinemann, 1985. – 320 p.

Отримана в редакції 09.02.2023, прийнята до друку 16.03.2023